Article

Cell PRESS

Interleukin-6 Is an Essential Regulator of Satellite Cell-Mediated Skeletal Muscle Hypertrophy

Antonio L. Serrano,[1,2] Bernat Baeza-Raja,[1,2] Eusebio Perdiguero,[1] Mercè Jardí,[1] and Pura Muñoz-Cánoves[1,*]
[1]Program on Differentiation and Cancer, Center for Genomic Regulation (CRG) and Center for Neurodegenerative Diseases (CIBERNED), Pompeu Fabra University, E-08003 Barcelona, Spain
[2]These authors contributed equally to this work.
*Correspondence: pura.munoz@crg.es

SUMMARY

Skeletal muscles adapt to increasing workload by augmenting their fiber size, through mechanisms that are poorly understood. This study identifies the cytokine interleukin-6 (IL-6) as an essential regulator of satellite cell (muscle stem cell)-mediated hypertrophic muscle growth. IL-6 is locally and transiently produced by growing myofibers and associated satellite cells, and genetic loss of *IL-6* blunted muscle hypertrophy in vivo. *IL-6* deficiency abrogated satellite cell proliferation and myonuclear accretion in the preexisting myofiber by impairing STAT3 activation and expression of its target gene cyclin D1. The growth defect was indeed muscle cell intrinsic, since *IL-6* loss also affected satellite cell behavior in vitro, in a STAT3-dependent manner. Myotube-produced IL-6 further stimulated cell proliferation in a paracrine fashion. These findings unveil a role for IL-6 in hypertrophic muscle growth and provide mechanistic evidence for the contribution of satellite cells to this process.

INTRODUCTION

Loss of muscle mass occurs in multiple settings, including cancer, AIDS, cachexia, and neuromuscular disorders, as well as during aging, remaining an important factor contributing to morbidity. Understanding the molecular pathways that regulate gain or loss of muscle mass is therefore crucial for treating muscle wasting-associated disorders. Positive modulation of skeletal muscle mass in response to increased workload results in hypertrophy of individual myofibers, but the key molecular mediators of this process are only beginning to be clarified (Glass, 2005).

Mounting evidence indicates that the endogenous adaptive growth capacity of mature myofibers is limited to a certain threshold due to the necessity of maintaining equilibrium between the increased cytoplasmic volume and the genetic machinery. Because multinucleated myofibers are permanently differentiated and are incapable of mitotic activity, the acquisition of new genetic material during postnatal muscle growth relies on accretion of new nuclei provided by a population of self-renewing muscle stem cells named satellite cells (Adams, 2006; Dhawan and Rando, 2005). Satellite cells, located in the muscle basal laminae, are quiescent but become activated to meet myofiber adaptive requirements. Indeed, if satellite cells' dividing capacity is ablated by local irradiation, increases in myonuclear number and full fiber hypertrophy do not occur in response to increased muscle loading (Adams et al., 2002; Rosenblatt and Parry, 1992; Rosenblatt et al., 1994). Once activated, satellite cells follow an ordered set of events, including proliferation, migration, and incorporation into the adult overloaded myofiber, leading to myofiber growth, in a process that can be partially recapitulated in vitro. In this context, although a number of secreted molecules have been implicated in the modulation of satellite cell behavior in vitro and ex vivo, the molecules controlling myonuclear accretion in the myofiber during the growth process in vivo remain basically unknown. Notably, autocrine/paracrine loops involving IGF-1 (insulin-like growth factor 1) are able to induce myofiber hypertrophy by activating PI3K (phosphatidylinositol 3-kinase)/AKT-dependent pathways (Bodine et al., 2001; Glass, 2005). The muscle-secreted cytokine interleukin-4 (IL-4) has been shown to promote muscle regeneration, a process which involves de novo myofiber formation, by specifically stimulating the fusion of myoblasts with myotubes (Horsley et al., 2003).

Interleukin-6 (IL-6) is a pleiotropic cytokine associated with the control and coordination of immune responses (Kishimoto, 2005). In addition to the classical cell types known to produce IL-6 (Kamimura et al., 2003), increasing evidence indicates that skeletal muscle cells are a further important source of IL-6 (Hiscock et al., 2004; Keller et al., 2001; Penkowa et al., 2003). In vitro studies have confirmed that IL-6 is produced by human primary myoblasts and murine C2C12 myogenic cells (Bartoccioni et al., 1994; De Rossi et al., 2000). Significantly, we have previously demonstrated that *IL-6* mRNA knockdown reduces muscle-specific gene expression in cultured C2C12 myoblasts (Baeza-Raja and Munoz-Canoves, 2004), suggesting a potential myogenic role for this cytokine. Since IL-6 is detected locally at elevated concentrations in actively contracting muscle fibers and after increased workload (Carson et al., 2002; Hiscock et al., 2004; Jonsdottir et al., 2000; Keller et al., 2001; Penkowa et al., 2003), both of which are known to induce satellite cell activities and stimulate an increase in muscle mass, we hypothesized a role for this cytokine in adult muscle growth. In this study, we first analyzed potential differences in growth capacity between muscles of *IL-6*^{+/+} (wild-type, WT) and *IL-6*^{−/−} (*IL-6*-deficient)
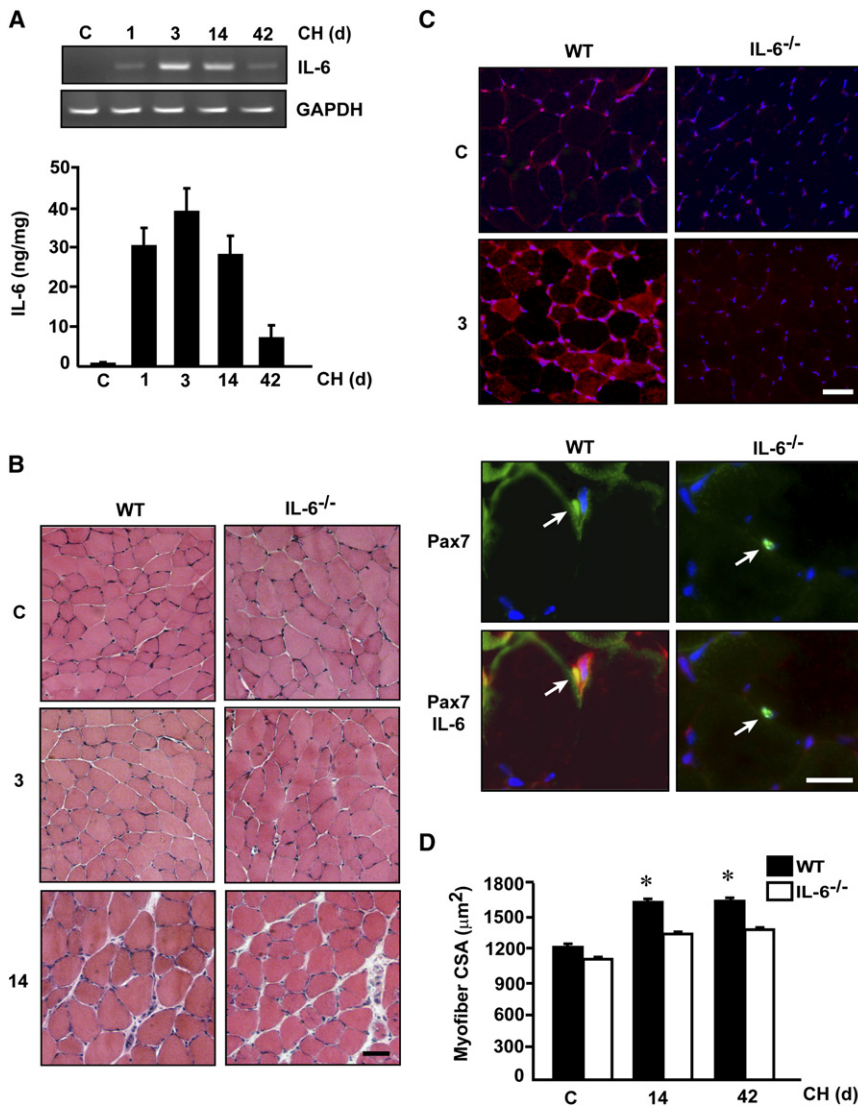
Figure 1. IL-6 Expression Is Induced during Hypertrophic Muscle Growth

Plantaris muscles from wild-type (WT) and $IL\text{-}6^{-/-}$ mice were obtained before surgery from nonoverloaded controls (C) and after the indicated number of days of compensatory hypertrophy (CH).

(A) Top: $IL\text{-}6$ expression was analyzed by RT-PCR. *Gapdh* expression was used as a control. Bottom: IL-6 protein expression was analyzed by ELISA. Concentration (mean ± SD) is expressed as ng/mg of total muscle protein extract.

(B) Representative images of plantaris muscle sections stained with hematoxylin and eosin from WT and $IL\text{-}6^{-/-}$ mice before (C) and after 3 and 14 days of CH. Scale bar = 50 μm.

(C) Top: immunostaining for IL-6 expression before (C) and after 3 days of CH in muscles from WT and $IL\text{-}6^{-/-}$ mice. Scale bar = 50 μm. Bottom: double immunolabeling for Pax7 (green) and IL-6 (red) in plantaris muscle sections after 3 days of CH. Arrows indicate Pax7-expressing cells. Scale bar = 20 μm.

(D) Mean cross-sectional area (CSA) of muscle fibers before (C) and after 14 and 42 days of CH in WT and $IL\text{-}6^{-/-}$ mice. Data are mean ± SEM. *$p < 0.05$ versus C.

tinued to be elevated after 3 and 14 days, decreasing thereafter (Figure 1A). Confirming the expected induction of muscle growth in this model, a significant increase in myofiber cross-sectional area (CSA) of the plantaris muscle was readily observed in comparison to control nonoverloaded muscles 14 days after overloading (Figure 1B, see WT panel). Next, we investigated the specific cellular source of IL-6 in skeletal muscle by immunohistochemistry. After overloading, IL-6 expression was clearly associated with both hypertrophying myofibers and mononucleated interstitial cells, including basal membrane-associated satellite cells, as shown by double labeling with specific antibodies for IL-6 and Pax7 (a satellite cell-specific marker) (Figure 1C). As a control, no IL-6 expression was detected in overloaded plantaris muscles from $IL\text{-}6^{-/-}$ mice (Figure 1C). Altogether, these results demonstrate a muscle-specific induction of IL-6 during hypertrophic growth.

To investigate the relevance of IL-6 in this process, we assessed potential differences in muscle growth between $IL\text{-}6^{-/-}$ and WT mice after overloading by morphometric analyses. Compared to WT mice, no significant increase in myofiber CSA was observed in $IL\text{-}6^{-/-}$ at 14 and 42 days after overloading (Figure 1D), indicating that IL-6 is necessary for myofiber hypertrophic growth. However, loss of $IL\text{-}6$ did not affect the baseline CSA of nonoverloaded plantaris myofibers (Figure 1D) or myofiber number (WT, 795 ± 132; $IL\text{-}6^{-/-}$, 751 ± 43; mean ± SD, $p > 0.05$), indicating that IL-6 is not required for muscle formation or basal maintenance of myofiber size.

mice after increasing mechanical load. Second, by using satellite cells derived from both WT and $IL\text{-}6^{-/-}$ muscles, we comparatively investigated their functional properties in response to IL-6. Based on our results, IL-6 emerges as an important molecule for muscle hypertrophy by controlling satellite cell proliferation and myonuclear accretion. Moreover, we uncover a role for the STAT3 activation pathway in mediating these effects.

RESULTS

IL-6 Deficiency Blunts Hypertrophic Muscle Growth

To investigate the putative role of IL-6 in skeletal muscle growth, we induced functional overloading of the mouse plantaris muscle by incapacitation of the gastrocnemius muscle and examined $IL\text{-}6$ expression during the process of compensatory hypertrophy (CH) of the plantaris at different time points. In nonoverloaded control muscles, $IL\text{-}6$ expression was almost undetectable at the mRNA and protein levels in the basal state (Figure 1A). In contrast, $IL\text{-}6$ expression was induced after 1 day of CH and con-
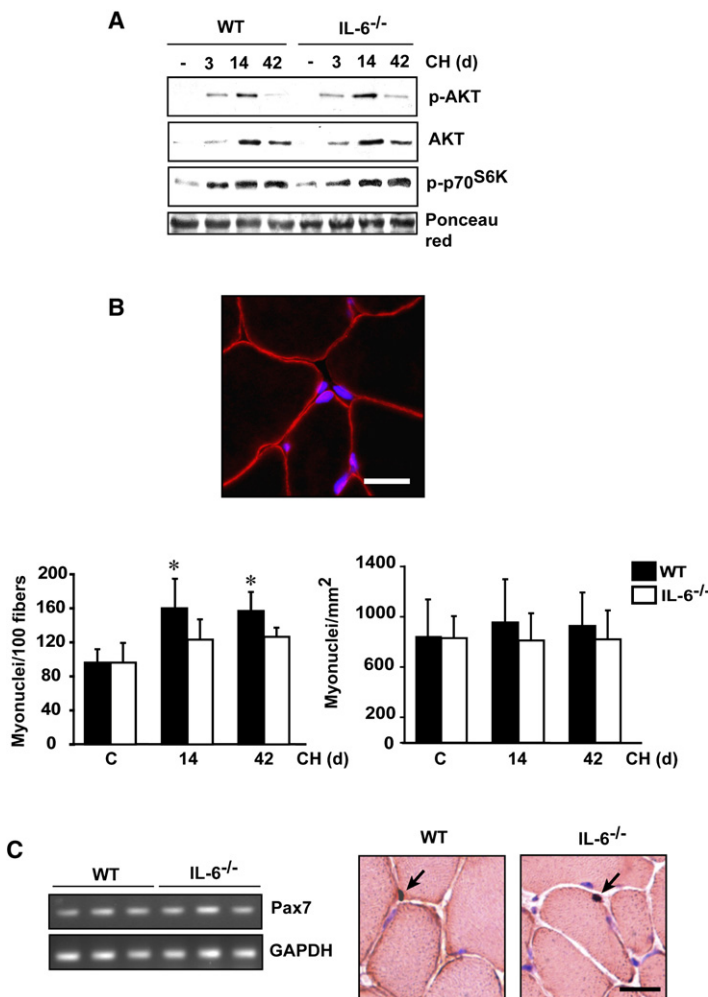
Figure 2. Myonuclear Accretion during Muscle Compensatory Hypertrophy Is Attenuated in IL-$6^{-/-}$ Mice

Plantaris muscles were obtained from WT and IL-$6^{-/-}$ mice before and after the indicated number of days of CH.

(A) Phosphorylated AKT, total AKT protein, and phosphorylated p70[S6K] were analyzed by western blotting using specific antibodies. Ponceau red was used as a loading control.

(B) Top: representative immunostaining for dystrophin (red) and nuclear staining with DAPI (blue) to illustrate myonuclear number assay. Scale bar = 20 μm. Bottom left: numbers of DAPI-stained nuclei within the dystrophin-positive sarcolemma were counted before (C) and after 14 and 42 days of CH and are expressed per 100 myofibers. Bottom right: the cytoplasm/nucleus ratio before and after muscle overloading is expressed as the number of DAPI-stained nuclei within the dystrophin-positive sarcolemma per mm^2. Data are mean ± SD. *$p < 0.05$ versus C.

(C) Left: $Pax7$ mRNA expression was analyzed by RT-PCR in control plantaris muscles from WT and IL-$6^{-/-}$ mice. $Gapdh$ mRNA expression was used as a control. Right: identification of satellite cells by Pax7 immunostaining (arrow) in control plantaris muscles. Scale bar = 20 μm.

paired increase in CSA of IL-$6^{-/-}$ myofibers results from defects in satellite cell-derived myonuclear accretion in the preexisting myofiber. Of note, the cytoplasm/nucleus ratio (expressed as myonuclei/mm^2) did not change significantly throughout the hypertrophic process (Figure 2B). In addition, no differences in satellite cell number at muscle basal state (as determined by quantification of Pax7-positive cells) were found between WT and IL-$6^{-/-}$ mice (satellite cells/100 fibers: WT, 2.27 ± 0,41; IL-$6^{-/-}$, 3.17 ± 0.06; mean ± SEM, p > 0.05). In agreement with this, $Pax7$ mRNA expression in control muscles from both genotypes was also similar (Figure 2C). These data provide direct in vivo evidence for the function of muscle-produced IL-6 in the myonuclear accretion occurring during myofiber hypertrophy.

Reduced Myonuclear Numbers in Overloaded IL-6-Deficient Myofibers

Since hypertrophic muscle growth is known to be regulated by protein synthesis pathways, such as the PI3K/AKT pathway (Glass, 2005), we comparatively analyzed the activation of AKT and its downstream mediator p70[S6K] in WT and IL-$6^{-/-}$ muscles at different time points during CH. As expected, both AKT expression and activation levels were induced during CH (Figure 2A); likewise, p70[S6K] was also activated during CH (Bodine et al., 2001) (Figure 2A). Notably, no differences in activated AKT and p70[S6K] were observed between overloaded muscles from WT and IL-$6^{-/-}$ mice, indicating that IL-6 is not required for the activation of the protein synthesis- and growth-associated PI3K/AKT pathway during CH and suggesting that IL-6 might affect satellite cell incorporation into hypertrophying myofibers. To this end, myonuclear number was assessed in control and overloaded WT and IL-$6^{-/-}$ plantaris muscle by determining the number of DAPI-stained nuclei within the dystrophin-stained sarcolemma (Figure 2B, top). A 40% increase in myonuclei number was observed in WT plantaris muscles at 14 days of CH and was maintained at 42 days, while no significant increase was observed in IL-$6^{-/-}$ muscles (Figure 2B), suggesting that the im-

IL-6 Loss Reduces Satellite Cell Proliferation

Since activation of satellite cells and their subsequent proliferation are necessary steps prior to the ultimate addition of myonuclei to growing myofibers (Darr and Schultz, 1989; Rosenblatt and Parry, 1993) and since local IL-6 induction occurred soon after overloading (at 1–3 days) (Figure 1A), we postulated that the reduced myonuclear number and CSA of IL-$6^{-/-}$ myofibers might result from defects at the early myogenic stages of the CH process in the absence of IL-6. To analyze the consequences of IL-6 loss on satellite cell activation and proliferation in vivo, we quantified the number of satellite cells expressing MyoD (a marker of activated satellite cells) and phosphorylated histone H3 (p-H3) (a marker of cells in S phase) in WT and IL-$6^{-/-}$ muscles 3 days after overloading. In basal conditions, the number of quiescent satellite cells was similar in both genotypes (see above), while no expression of MyoD was detected in WT or IL-$6^{-/-}$ muscles (data not shown). Muscle overloading induced the activation of satellite cells, as detected by the induced expression of MyoD with respect to control muscles, to a similar extent in both genotypes (Figure 3A). However, the number of cells double-positive for MyoD and p-H3 was severely reduced in IL-$6^{-/-}$ overloaded muscles (Figure 3B). Confirming the
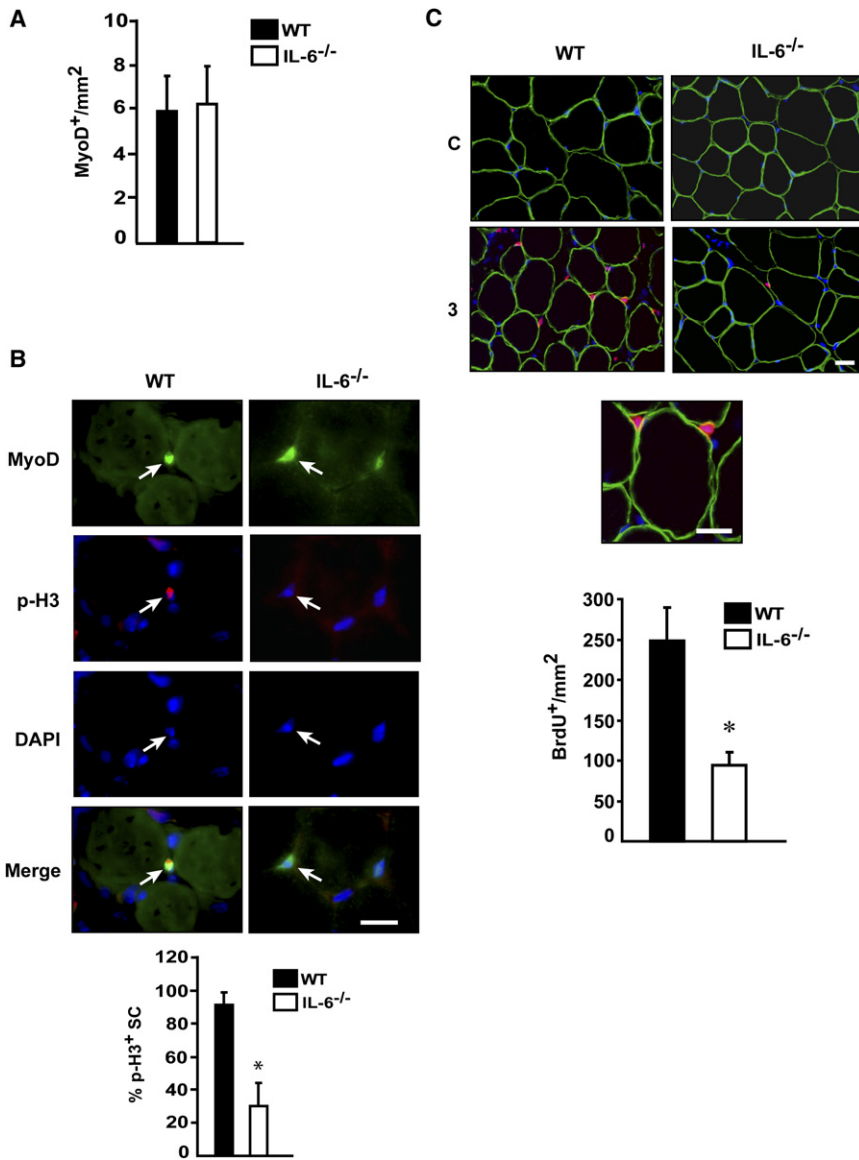
A

C

B

Figure 3. Loss of *IL-6* Reduces Satellite Cell Proliferation after Muscle Overloading

Sections of plantaris muscles obtained from WT and *IL-6*$^{-/-}$ mice 3 days after overloading were immunostained with antibodies against MyoD and phosphorylated histone H3 (p-H3). Nuclei were detected with DAPI.

(A) Quantification of the number of MyoD-positive cells per mm^2. Data are mean ± SD.

(B) Top: double immunostaining for MyoD (green) and p-H3 (red) in muscle sections. Scale bar = 20 μm. Bottom: percentage of total MyoD-positive cells coexpressing p-H3 in both genotypes. Arrows indicate MyoD-positive cells. Data are mean ± SD.

(C) Top: double immunostaining for BrdU (red) and dystrophin (green) and nuclear staining with DAPI (blue) in muscle sections from WT and *IL-6*$^{-/-}$ mice before (C) and after 3 days of CH. Middle: higher magnification of BrdU and dystrophin immunostaining is shown. Bottom: BrdU-positive cells per mm^2 were quantified in WT and *IL-6*$^{-/-}$ plantaris muscle sections after 3 days of CH. Scale bar = 20 μm. Data are mean ± SEM.
*$p < 0.05$ versus WT.

myotubes in vitro (see Figures S1A and S1B available online), in agreement with the in vivo expression in satellite cells and growing myofibers (Figure 1C). Since no clear evidence for the presence of the IL-6 receptor complex in muscle cells has yet been provided, we investigated the expression of the IL-6 receptor complex components gp130 and IL-6Rα in muscle cells. Indeed, transcripts of both components as well as membrane-bound IL-6Rα protein were expressed in primary and C2C12 muscle cells (Figures S1C–S1E). Interestingly, *IL-6* loss did not affect the expression of IL-6Rα in *IL-6*-deficient cells (Figures S1E and S1F). Furthermore, IL-6Rα was also detected in plantaris muscle membrane extracts (Figure S1G). Additionally, we demonstrate that shedding of the receptor, which has been reported in other cell types (Rose-John, 2003), also occurs in muscle cells. Indeed, western blotting analysis of primary and C2C12 myoblast cell culture media and plantaris muscle extracts revealed the presence of the soluble 50 kDa IL-6Rα (sIL-6Rα) (Figures S1H and S1I). Thus, IL-6 may signal in muscle cells through both the cell-surface-associated and soluble forms of IL-6Rα.

Based on the synthesis of IL-6 by both satellite cells and growing myofibers in vivo, we hypothesized potential autocrine and/or paracrine actions of IL-6 on satellite cell proliferation. To address the autocrine role of IL-6, we analyzed the differences in proliferation rates between WT and *IL-6*$^{-/-}$ myoblasts by determining the incorporation of BrdU. *IL-6*$^{-/-}$ cells exhibited an ~50% reduction in the rate of proliferation compared to WT cells (Figure 4A); importantly, the proliferation deficit was rescued by addition of recombinant IL-6 (rIL-6). This result argued against
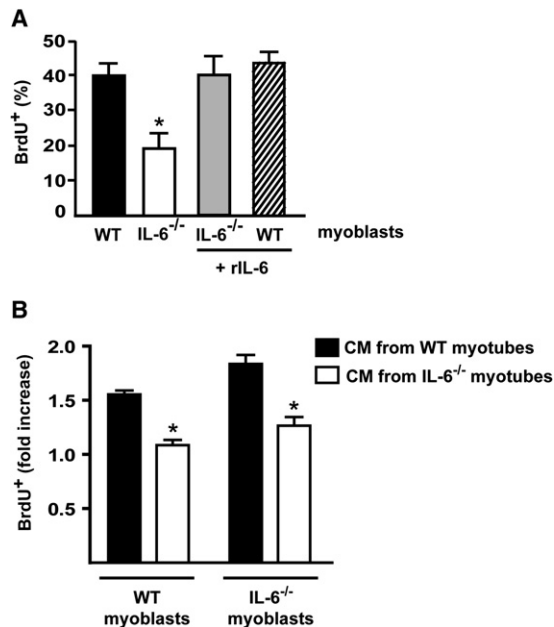
defective proliferation in the absence of *IL-6*, bromodeoxyuridine (BrdU) administration to *IL-6*$^{-/-}$ and WT mice after overloading showed cells in S phase (BrdU$^+$) outside of the dystrophin outline in plantaris muscle of both WT and *IL-6*$^{-/-}$ mice at 3 days after overloading, but not in control nonoverloaded muscles; notably, the number of BrdU-positive cells was strongly reduced in the absence of *IL-6* after CH (Figure 3C). Together, these data demonstrate that IL-6 is dispensable for satellite cell activation but is critical for satellite cell proliferation during CH; hence, the impaired proliferation in the absence of *IL-6* may impede new myonuclear accretion in growing myofibers.

IL-6 Regulates Myoblast Proliferation and Migration

To further investigate whether the in vivo growth defects in the absence of *IL-6* are muscle cell intrinsic, we examined satellite cell-derived primary myoblast functions in vitro. RT-PCR and ELISA analyses showed that IL-6 transcript and protein were expressed by proliferating primary myoblasts and by growing

Figure 4. IL-6 Is Necessary for Myoblast Proliferation
Satellite cell-derived primary myoblasts from WT and $IL-6^{-/-}$ mice were analyzed.
(A) Percentage of BrdU-positive cells in WT and $IL-6^{-/-}$ primary myoblasts treated without (left two columns) or with (right two columns) rIL-6. *$p < 0.05$ versus untreated WT.
(B) Relative proliferation rates of WT and $IL-6^{-/-}$ myoblasts in the presence of conditioned medium (CM) from WT or $IL-6^{-/-}$ myotubes, expressed as proliferation rate with respect to each cell type in the presence of nonconditioned medium, which was arbitrarily given a value of 1. *$p < 0.05$ versus control. Data are mean ± SD.

a possible nonspecific effect derived from the deletion of the *IL-6* gene in myoblasts. Furthermore, C2C12 myoblasts stably expressing IL-6 (C2/IL-6) also exhibited a higher proliferation rate than mock-transfected C2C12 cells (Figure S2A). The potential paracrine action of growing myofiber-produced IL-6 on satellite cell proliferation was addressed in vitro by determining the BrdU incorporation rate of $IL-6^{-/-}$ myoblasts in response to conditioned medium (CM) from WT and $IL-6^{-/-}$ growing myotubes. CM from $IL-6^{-/-}$ myotubes stimulated myoblast proliferation to a lesser extent than CM from WT myotubes (Figure 4B). Thus, IL-6 is necessary for adequate myoblast proliferation in vitro, in agreement with the in vivo proliferation defect observed in overloaded muscles of *IL-6*-deficient mice. Moreover, these findings underscore the contribution of both myoblast- and myofiber-produced IL-6 to the proliferation of muscle cells during the growth process.

Proliferating satellite cells must migrate and establish stable cell-fiber contacts for accretion of myonuclei. Thus, we analyzed the contribution of IL-6 to myoblast migration by using standard transwell migration assays. As shown in Figure S3A, migration of primary myoblasts from $IL-6^{-/-}$ mice was reduced compared to WT cells, while supplementation with rIL-6 rescued this defect. The extent of migration was also higher in C2/IL-6 myoblasts compared to C2C12 control cells (Figure S3B). Moreover, CM from WT myotubes stimulated the migration of WT or $IL-6^{-/-}$ myoblasts to a greater extent than $IL-6^{-/-}$ myotube CM (Fig-

ure S3C). These in vitro results support the idea that migratory defects of myoblasts in the absence of *IL-6* may also contribute to the reduced myonuclear number and size of overloaded fibers in *IL-6*-deficient mice.

Role of STAT3 in IL-6-Induced Myoblast Proliferation and Migration

To gain mechanistic insights into how IL-6 controls myoblast functions, we first examined potential differences in the activation of IL-6-responsive signaling pathways in WT and $IL-6^{-/-}$ myoblasts. ERK and PI3K/AKT pathways have been previously implicated in myogenesis (Forcales and Puri, 2005; Mourkioti and Rosenthal, 2005), and both pathways can be activated by IL-6 in certain cell types (Ernst and Jenkins, 2004). On the other hand, the JAK/STAT3 pathway is a major route activated by IL-6, especially in inflammatory cells (Kamimura et al., 2003), although its implication in myogenesis has remained unclear. We therefore analyzed the activation of these three pathways in myoblasts expressing or lacking *IL-6* using anti-phosphospecific antibodies for the activated forms of ERK, AKT, and STAT3, respectively. The levels of activated STAT3 were much lower in $IL-6^{-/-}$ myoblasts than in WT cells, and, importantly, they were rescued by exogenous rIL-6 (Figure 5A), indicating a muscle-intrinsic modulation of STAT3 activity by IL-6. Addition of rIL-6 (Figure 5A) or CM from WT myotubes (data not shown) further increased the activation of STAT3 in WT myoblasts, supporting the idea of a paracrine action of IL-6 in myoblast signaling via STAT3. At variance with these results, no significant differences in ERK and AKT activation were detected between cells expressing or lacking *IL-6* or in response to exogenous IL-6 (Figure 5A). These results suggested that the activation of STAT3—rather than activation of AKT and ERK—by IL-6 could underlie its control of myoblast proliferation and migration.

To test this possibility, WT myoblasts were cultured in the absence or presence of AG490, an inhibitor of the JAK/STAT3 pathway, and wortmannin, an inhibitor of the PI3K/AKT pathway (used as a negative control) (Figure S4), and cell proliferation and migration rates were determined. The effects of both inhibitors on exogenous IL-6-induced myoblast proliferation and migration were also examined in parallel assays. AG490, but not wortmannin, blocked myoblast proliferation and migration both in WT myoblasts and in rIL-6-treated WT and $IL-6^{-/-}$ myoblasts (Figure 5B; Figure S4B); also, the effect of WT myotube CM on myoblast proliferation and migration was blunted by AG490, but not by wortmannin (Figure 5C; Figure S4C), suggesting that STAT3 activation is a major contributor to the autocrine and paracrine effects of IL-6 on myoblast proliferation and migration.

To confirm the direct and specific role of STAT3 activation in these IL-6-mediated processes, we used two independent approaches consisting of retroviral overexpression of a dominant-negative form of STAT3 (STAT3D) and cell treatment with a specific inhibitory peptide for STAT3 dimerization (STAT3pi) (Turkson et al., 2001). Both STAT3D and STAT3pi reduced the proliferation and migration of WT myoblasts and of $IL-6^{-/-}$ myoblasts treated with rIL-6 or with CM from WT myotubes (Figures 5D and 5E; Figures S4D–S4G). Thus, if STAT3 mediates the IL-6 effect on myoblast proliferation, the ectopic expression of a constitutively active form of STAT3 (STAT3C) should be sufficient to rescue the proliferation and migration defect of myoblasts
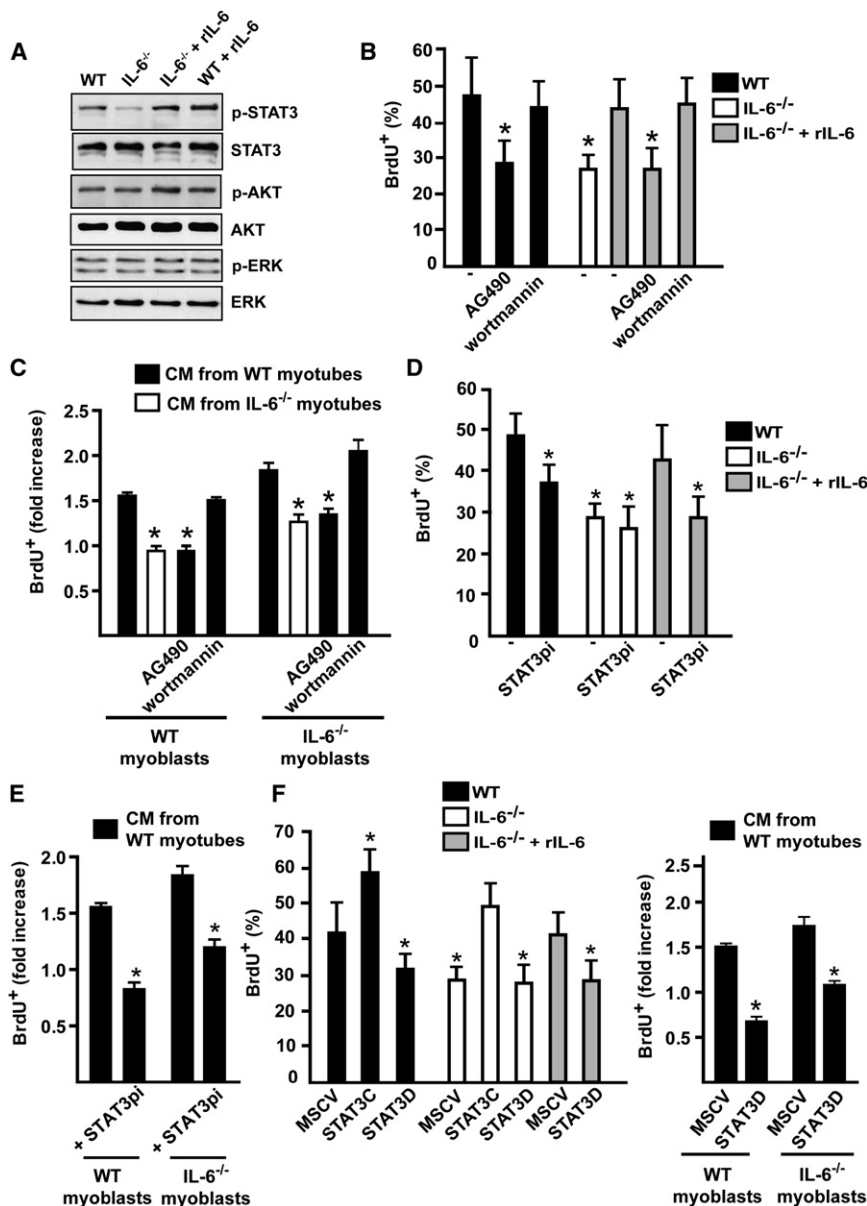
Figure 5. Reduced Activation of the STAT3 Pathway Underlies the Proliferation Defect of Myoblasts in the Absence of *IL-6*

(A) Activation of the STAT3, AKT, and ERK signaling pathways was analyzed in WT and $IL-6^{-/-}$ primary myoblasts, treated with or without rIL-6, by western blotting using specific antibodies against their phosphorylated forms.

(B) Percentage of BrdU-positive WT and $IL-6^{-/-}$ primary myoblasts treated with or without rIL-6 in the absence or presence of AG490 and wortmannin as indicated.

(C) Relative proliferation rates of WT and $IL-6^{-/-}$ myoblasts in the presence of CM from WT or $IL-6^{-/-}$ myotubes, treated with or without AG490 and wortmannin where indicated, and expressed as proliferation rate with respect to each cell type in the presence of nonconditioned medium, which was arbitrarily given a value of 1.

(D) Percentage of BrdU-positive WT and $IL-6^{-/-}$ primary myoblasts treated with or without rIL-6 in the absence or presence of a STAT3 inhibitor peptide (STAT3pi) as indicated.

(E) Relative proliferation rates of WT and $IL-6^{-/-}$ myoblasts in the presence of CM from WT myotubes, treated with or without STAT3pi where indicated, and expressed as proliferation rate with respect to each cell type in the presence of nonconditioned medium, which was arbitrarily given a value of 1.

(F) Percentage of BrdU-positive WT and $IL-6^{-/-}$ primary myoblasts treated with or without rIL-6 (left) or with CM from WT myotubes (right) in the presence of a retroviral vector encoding a constitutively active (MSCV-STAT3C) or negative (MSCV-STAT3D) form of STAT3. Empty vector (MSCV) was used as a control.

Data in (B)–(F) are mean ± SD. *$p < 0.05$ versus control WT in (B), (D), and left panel of (F); *$p < 0.05$ versus each cell type in (C), (E), and right panel of (F).

lacking *IL-6*. Indeed, retroviral expression of STAT3C in $IL-6^{-/-}$ myoblasts restored their proliferation and migration rates to levels similar to those of WT cells (Figure 5F; Figures S4F and S4G). Moreover, the proliferation and migration of WT myoblasts were further enhanced by STAT3C (Figure 5F; Figure S4F). These results demonstrate that IL-6 produced by myoblasts or myotubes induces activation of STAT3, which is then required for efficient myoblast proliferation and migration.

IL-6 and STAT3 Control Myoblast Proliferation Gene Expression

Since STAT3 binding sites have been described in the promoters of myoblast proliferation-associated cyclin D1 (*Ccnd1*) and c-*myc* genes (Endo and Nadal-Ginard, 1986; Kiuchi et al., 1999; Masuda et al., 2002; Wei and Paterson, 2001), we postulated that their expression in myoblasts could be modulated by

IL-6. RT-PCR analysis showed that cyclin D1 and c-*myc* levels were reduced in myoblasts lacking *IL-6* compared to WT myoblasts, and importantly, their levels were rescued by addition of rIL-6 (Figure S5A) or CM from WT myotubes (data not shown). To confirm that STAT3 activation specifically mediated the IL-6-induced expression of these genes in proliferating myoblasts, we analyzed their transcript levels in the presence or absence of STAT3-specific inhibitors and activators. Retroviral delivery of STAT3D and treatment with STAT3pi or AG490 reduced the expression of cyclin D1 and c-*myc* both in WT myoblasts and in rIL-6-treated $IL-6^{-/-}$ myoblasts (Figures S5B and S5C); conversely, infection of *IL-6*-deficient myoblasts with STAT3C rescued the lower expression of both genes (Figure S5C). No effect was observed by addition of wortmannin (Figure S5B). Thus, IL-6 is necessary for myoblast proliferation via activation of the STAT3 pathway, which in turn controls the expression of key cell

proliferation regulators such as cyclin D1 and c-*myc*. The expression of myoblast migration-associated gene products such as the uPA receptor, uPAR (*Plaur*), and fibronectin (*Fn1*), whose promoters harbor STAT3 binding sites and/or are regulated by IL-6 (Birchmeier and Brohmann, 2000; Bonavaud et al., 1997; Turner et al., 1983; Wells and Strickland, 1997), was also reduced in *IL-6*-deficient myoblasts compared to WT myoblasts and was upregulated by the addition of rIL-6 (Figure S5D), suggesting that their reduced expression may underlie, at least in part, the migration defect of myoblasts lacking *IL-6*.

The IL-6/STAT3 Axis Regulates Satellite Cell Response to Muscle Overloading

Based on the defective satellite cell proliferation after muscle overloading in *IL-6*-deficient mice (see Figure 3B), we aimed to confirm the relevance of the IL-6/STAT3 axis in the proliferation of satellite cells during compensatory muscle growth. To this end, we analyzed STAT3 activation in overloaded muscles of WT and *IL-6*$^{-/-}$ mice using both western blotting and immunohistochemical approaches. STAT3 expression and activation levels were induced during CH in both genotypes as reflected by immunoblotting assays (Figure S6A). In contrast, immunohistochemical analysis revealed that the number of satellite cells coexpressing MyoD and activated STAT3 was significantly reduced in *IL-6*$^{-/-}$ muscle 3 days after overloading (Figure 6), in accordance with the reduced presence of satellite cells coexpressing MyoD and the proliferation marker p-H3 (see Figure 3B). These results are in agreement with the in vitro data demonstrating that IL-6 induces satellite cell proliferation through the activation of the STAT3 pathway. Accordingly, *IL-6* loss resulted in reduced expression of the proliferation- and migration-associated STAT3 target genes cyclin D1 and fibronectin in plantaris muscles 3 days after overloading (Figure 7A). Together, these results indicate that loss of *IL-6* results in normally activated satellite cells that fail to proliferate early after the hypertrophic stimulus (3 days).

We next investigated the myogenic progression of satellite cells from both WT and *IL-6*$^{-/-}$ mice during the course of the hypertrophic growth process, at days 0, 3, 5, 7, 9, and 14 after overloading (Figure S7). We found that the number of satellite cells expressing the activation marker MyoD increased at the earliest time point after overloading in both WT and *IL-6*-deficient muscles (Figure 3A; Figure S7). Importantly, while the number of satellite cells expressing MyoD increased at later time points after overloading (5 and 7 days) in WT muscle in a proficient proliferative response, no increase was observed in the absence of *IL-6* (Figure S7), in agreement with the defective proliferation of *IL-6*-deficient myoblasts in vitro. Reinforcing these data, no increase in BrdU-positive cells was detected in *IL-6*-deficient muscle at later time points after overloading (in conditions of daily BrdU administration; data not shown), suggesting a persistent block of cell proliferation in the absence of *IL-6*. In addition, the time-dependent myogenic progression of satellite cells to further differentiation stages was compromised in overloaded muscles lacking *IL-6*, as evidenced by the impaired increase in myogenin- and embryonic myosin heavy chain (eMHC)-positive cells already detectable at early stages (Figures 7B and 7C; Figure S7) and at late points after overloading (Figure S7) compared to WT muscles. These results suggest that, in the absence of *IL-6*, the deficient satellite cell differentiation after muscle overloading
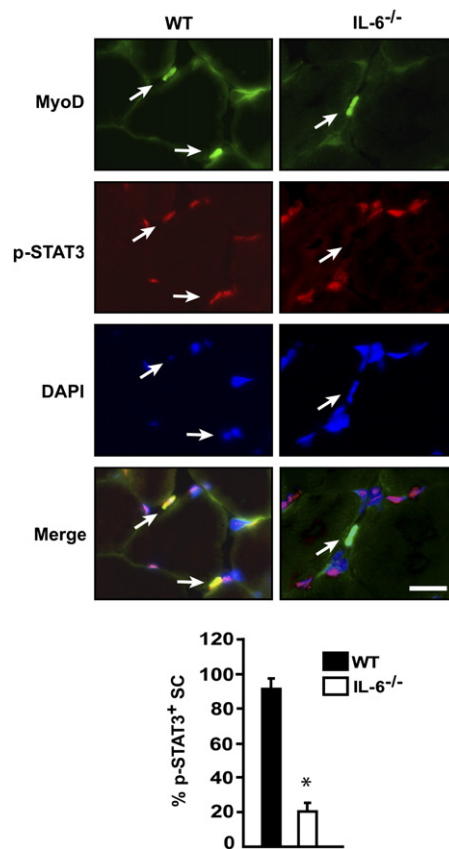

Figure 6. Loss of *IL-6* Reduces STAT3 Activation after Muscle Overloading

Sections of plantaris muscles obtained from WT and *IL-6*$^{-/-}$ mice after 3 days of overloading were immunostained with antibodies against MyoD and p-STAT3. Nuclei were detected with DAPI. Top: double immunostaining for MyoD (green) and p-STAT3 (red) in overloaded muscles, illustrating the different coexpression patterns in muscles from WT and *IL-6*$^{-/-}$ mice. Arrows indicate MyoD-positive cells; scale bar = 20 μm. Bottom: percentage of total MyoD-positive cells coexpressing p-STAT3 in both genotypes. Data are mean ± SD. *p < 0.05 versus WT.

may be a consequence of the cell proliferation block, thereby resulting in the abrogation of myofiber growth.

Altogether, these data demonstrate that *IL-6* loss results in deficient STAT3 signaling in activated satellite cells, leading to their reduced proliferation and myogenic progression, and highlight the major role played by the IL-6/STAT3 axis in controlling these processes during compensatory hypertrophy.

DISCUSSION

The principal finding of this study is that IL-6 plays a critical role in skeletal muscle hypertrophic growth. Our results have evidenced that (1) skeletal muscle fibers strongly induce the local, transient expression and release of IL-6 in response to a hypertrophic stimulus; (2) muscle-produced IL-6 regulates muscle growth in vivo, as shown by the blunted increase of myofiber size in a compensatory hypertrophy model in *IL-6*-deficient mice; (3) the defective growth is due to impaired proliferation—and migration—of satellite cells (muscle stem cells) affecting the subsequent myonuclear
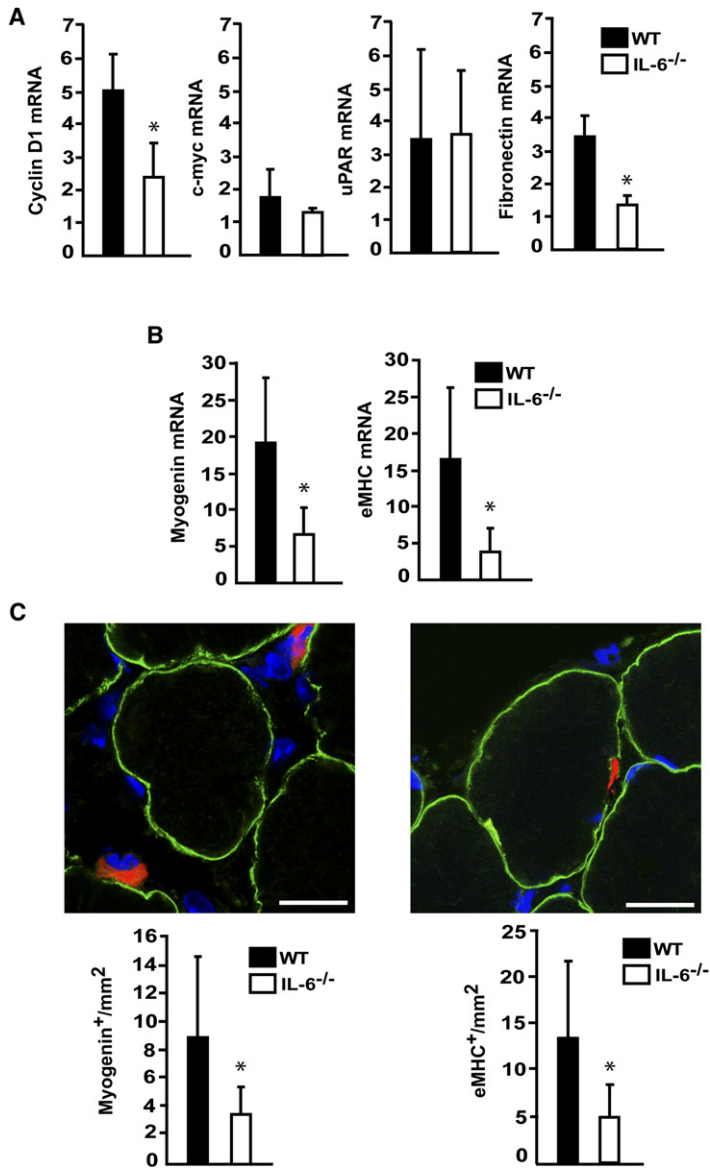
Figure 7. Expression of Proliferation-, Migration-, and Differentiation-Associated Genes Is Reduced in *IL-6*$^{-/-}$ Muscles after Overloading

Plantaris muscle sections and mRNA were obtained from WT and *IL-6*$^{-/-}$ mice before and after 3 days of CH.

(A) Cyclin D1 (*Ccnd1*), c-*myc*, uPAR (*Plaur*), and fibronectin (*Fn1*) mRNA expression levels were analyzed by qRT-PCR. Data are expressed as fold induction relative to control WT muscle.

(B) Myogenin (*Myog*) and eMHC (*Myh3*) mRNA expression levels were analyzed by qRT-PCR. Data are expressed as in (A).

(C) Top: Representative confocal images of myogenin- and eMHC-positive cells (red) in WT overloaded muscles. Myofiber outline is shown by dystrophin staining (green), and nuclei are stained with DAPI (blue). Scale bar = 25 μm. Bottom: quantification of myogenin- and eMHC-positive cells in both genotypes.

Data are mean ± SD. *$p < 0.05$ versus WT.

accretion in the preexisting myofiber; (4) the growth defect is indeed muscle cell intrinsic since loss of *IL-6* results in reduced satellite cell-derived myoblast proliferation and migration, while exogenously added IL-6 rescues these defects, and more importantly, myotube-produced IL-6 also stimulates myoblast proliferation and migration, demonstrating autocrine and paracrine actions of IL-6 on muscle growth; and (5) the STAT3 pathway emerges as the main effector of the growth-promoting action of IL-6 on muscle cells by controlling the expression of proliferation- and migration-associated STAT3 target genes. These findings provide insights into the mechanisms regulating the contribution of satellite cells to physiological hypertrophy in adult muscles. Notably, the beneficial function of local and transiently produced IL-6 is opposed to the known muscle-wasting effect of infused IL-6 or systemic high levels of IL-6 in cachectic conditions (Haddad et al., 2005; Tisdale, 2005).

Skeletal muscles adapt to changes in their workload and activity by modifying their fiber size. The activation of the AKT/mTOR

pathway and its downstream targets p70^{S6K} and 4E-BP1 by controlling net protein content is a crucial regulator of skeletal muscle hypertrophic growth (Bodine et al., 2001; Glass, 2003, 2005). Increasing evidence also demonstrates that muscle hypertrophy is associated with and dependent on the addition of new myonuclei via the proliferation and further fusion of satellite cell-derived myoblasts to the adult myofiber (Dhawan and Rando, 2005; O'Connor et al., 2007). However, the extracellular factors and downstream molecular signaling pathways responsible for satellite cell-mediated hypertrophy have not been yet identified. The expression of IL-6 (a cytokine classically associated with the control of immune responses) is induced in response to increased workload (Carson et al., 2002) and skeletal muscle contraction during exercise (Pedersen and Fischer, 2007); however, its potential role in muscle hypertrophy was unknown. Our results show that IL-6 expression is induced in growing myofibers and associated satellite cells during compensatory hypertrophy. Moreover, we demonstrate that *IL-6* deficiency results in blunted myofiber hypertrophic growth due to impaired satellite cell proliferation and further incorporation into preexisting myofibers after overloading in vivo. Significantly, *IL-6* gene deletion did not produce a reduction of fiber size in adult mice in the basal state, indicating that the mechanisms involved in maintenance of fiber size in mature muscles are IL-6 independent. Elegant studies by Horsley et al. (2003) have previously demonstrated that the cytokine IL-4 controls new myofiber formation during injury-induced muscle regeneration, a process recapitulating embryonic myogenesis, which is mechanistically different from physiological adaptive growth of preexisting normal myofibers in adult muscle (as in this study). Horsley et al. (2003) found that during new myofiber formation, IL-4 acts exclusively at the level of myoblast fusion with nascent myotubes, without affecting prior myogenic stages. We show that IL-6 controls satellite cell proliferation and migration, and hence their ulterior incorporation to the hypertrophying myofiber, suggesting different roles and mechanisms of action of both cytokines in distinct skeletal muscle processes.

A previous immunohistochemical study described STAT3 activation during injury-induced muscle inflammation and regeneration; however, this was ascribed to an IL-6-independent action (Kami and Senba, 2002). Our results demonstrate that the levels of activated STAT3, the primary STAT protein activated by ligation of the IL-6 receptor (Kamimura et al., 2003; Kishimoto, 2005), are significantly reduced in *IL-6*-deficient myoblasts in vitro. More importantly, STAT3 activation was also reduced in satellite cells from IL-$6^{-/-}$ muscles in vivo in response to overloading. We demonstrate that the reduced activation of STAT3 underlies the proliferation and migration defects of myoblasts lacking *IL-6*, while ectopic activation of STAT3 restores both processes. In accordance with our results, activation of STAT3 by LIF, an IL-6 family member, has been shown to be essential for stem cell self-renewal (Dani et al., 1998), while hyper-IL-6, a fusion protein of soluble IL-6R and IL-6 that signals via gp130 homodimer receptors, can also sustain embryonic stem cell self-renewal (Viswanathan et al., 2002).

We identified cyclin D1 as a STAT3 target gene product downregulated in satellite cells from *IL-6*-deficient muscle in vitro and in vivo. Cyclin D1 is necessary for proliferation of different cell types, including myogenic cells; in particular, myoblast proliferation and cell-cycle exit are critically dependent on the regulation of the cyclin D1 gene in response to cellular growth signals (Kitzmann and Fernandez, 2001; Rao et al., 1994; Wei and Paterson, 2001). Thus, the reduced proliferation of myoblasts in the absence of *IL-6* could be attributed to the reduced expression of cyclin D1. Indeed, forced activation of STAT3 restored cyclin D1 expression in IL-$6^{-/-}$ myoblasts concomitantly with their proliferation capacity. Previous reports have demonstrated a regulatory role for the NF-κB and JNK/c-Jun pathways (Guttridge et al., 1999; Perdiguero et al., 2007) in cyclin D1 gene transcription in myoblasts in vitro. Our results provide an additional mechanism underlying cyclin D1 gene expression in proliferating myoblasts both in vitro and in vivo, via IL-6-induced STAT3 activation. Besides controlling muscle-specific gene expression, the myogenic regulator MyoD can induce growth arrest in normal and transformed cells independently of differentiation, at least in part by inducing expression of the p21 gene (*Cdkn1a*) (Crescenzi et al., 1990; Halevy et al., 1995; Sorrentino et al., 1990; Wei and Paterson, 2001). An interaction of MyoD with STAT3 resulting in impaired MyoD-mediated activities has been previously reported in cell overexpression experiments (Kataoka et al., 2003). Thus, in addition to downregulating cyclin D1, loss of *IL-6* may promote the myoblast growth-arresting function of MyoD by restraining it from the inhibitory action of STAT3. Supporting this possibility, the expression of the MyoD-inducible *p21* gene was induced in IL-$6^{-/-}$ myoblasts in vitro and in overloaded IL-$6^{-/-}$ muscles (see Figure S6B), which may contribute to the observed reduced muscle cell proliferation. On the other hand, migration of myoblasts in response to IL-6/STAT3 may also constitute a necessary step for their incorporation into the preexisting myofiber, leading to muscle growth, at least in part by regulating the expression of the migration-associated gene products fibronectin and uPAR. Interestingly, migratory functions have also been attributed to cyclin D1 (Li et al., 2006) in addition to its classical cell-cycle-controlling role (Kitzmann and Fernandez, 2001), thus suggesting that cyclin D1 may also contribute to the promigratory action of IL-6 during muscle growth.

The fact that IL-6 is produced not only by proliferating satellite cells but also by growing myofibers during hypertrophy in vivo suggests that IL-6 may also impact satellite cell proliferation—and migration—during compensatory growth in a paracrine fashion. Indeed, IL-6 produced by growing myotubes (and exogenous recombinant IL-6) stimulated the proliferative potential of myoblasts in vitro. Most importantly, loss of *IL-6* in overloaded muscles prevents satellite cell myogenic progression, since the normal transition of satellite cells from a proliferative to a differentiated state is hampered during the hypertrophic process. We further demonstrated that satellite cells can be normally activated after hypertrophic stimulus in the absence of *IL-6*, as evidenced by the similar number of MyoD-expressing cells at 3 days after overloading; however, they are incapable of further proliferating and differentiating at subsequent stages during the progression of the muscle growth process. Our results lead us to propose that the reduced STAT3 activation in satellite cells of *IL-6*-deficient muscles after overloading may play a causal role in the subsequent block of satellite cell myogenic progression. Interestingly, since IL-6 production by nerve-mediated skeletal muscle contraction has recently been shown to be partly dependent on the activation of the calcineurin pathway (Banzet et al., 2007) and since calcineurin is a major mediator of nerve activity on muscle gene expression (Schiaffino and Serrano, 2002), IL-6 may play a role as a factor released in response to neural influences that promotes contraction-induced muscle growth.

Taken together, the results of this study demonstrate that IL-6 is necessary for adult hypertrophic muscle growth in vivo and unveil a role for muscle-produced IL-6 as a major regulator of satellite cell proliferation and myonuclear accretion. More importantly, our data uncover the IL-6/STAT3 axis as a critical mechanism underlying satellite cell proliferation-mediated hypertrophic muscle growth. This mechanism is distinct from previously known adult muscle cell-autonomous endogenous pathways, which stimulate protein synthesis. By identifying a pathway responsible for controlling skeletal muscle hypertrophy, this work carries potential significance for the search for muscle atrophy therapies.

EXPERIMENTAL PROCEDURES

Animals

IL-$6^{-/-}$ mice, produced on the 129SvJ × C57BL/6 background (WT) and generated by heterozygous mating of mice carrying a targeted disruption in which the second exon in the *IL-6* gene was replaced by a *neo*^{r} cassette (Kopf et al., 1994), were generously provided by A. Bernad (Centro Nacional de Investigaciones Cardiovasculares, Madrid). Mouse genotypes were confirmed by PCR analysis of tail genomic DNA (Kopf et al., 1994). In vivo studies were performed using male mice between 8 and 12 weeks of age.

Induction of Compensatory Muscle Growth

Animals were anesthetized with ketamine/xylazine (80/10 mg/kg, intraperitoneally), and compensatory hypertrophy (CH) of plantaris muscles was induced by surgical section of the distal tendon of the medial and lateral gastrocnemius muscle, which was folded back and sutured close to its proximal origin. This procedure induces an adaptive growth response to functional overloading in the soleus and plantaris muscles. Sham-operated limbs were used as controls. In some experiments, to investigate cell proliferation during compensatory hypertrophy, 30 mg/kg/day BrdU (Sigma) in saline solution was injected intraperitoneally for 2 days. At the indicated times, animals were sacrificed and muscles were dissected, frozen in isopentane cooled with liquid nitrogen, and stored at −80°C until analysis. A minimum of five animals of each genotype were

analyzed for every experiment and time point studied. All animal experiments were approved by the Catalan government Animal Care Committee.

Cell Culture
C2C12, IL-6-overexpressing C2C12 (C2/IL-6), and RAW264.7 cell lines were cultured as described in Supplemental Data. Satellite cell-derived primary myoblasts were obtained from muscles of WT and IL-$6^{-/-}$ mice. Myoblast isolation and culture were performed as described in Supplemental Data.

Reagents
Recombinant IL-6 (rIL-6, Peprotech; 10 ng/ml), a specific STAT3 inhibitor peptide (STAT3pi, Calbiochem; 500 μM), a JAK/STAT inhibitor (AG490, Sigma; 50 μM), and a PI3K inhibitor (wortmannin, Sigma; 1 μM) were added to growth medium (GM) or differentiation medium (DM) where indicated.

Transfections
For the generation of the stably transfected IL-6-overexpressing C2C12 cell line (C2/IL-6), cells were transfected with the pBM6DraA6 (IL-6) expression vector using Lipofectamine (Invitrogen) as described previously (Baeza-Raja and Munoz-Canoves, 2004), and pools of G418-resistant colonies were selected.

Proliferation
To detect S phase cells, cultures were pulsed with BrdU (Sigma) for 1 hr and then processed and analyzed as described in Supplemental Data.

Migration Assays
To analyze cell migration ability, cultures were incubated in transwells and then processed and quantified as described in Supplemental Data.

ELISA
Both primary and C2C12 myoblasts were cultured in GM (proliferating myoblasts) and for 48 hr in DM (myotubes). For the detection of IL-6 in cell culture media and muscle extracts, an ELISA kit (BD Biosciences) was used according to the manufacturer's instructions.

Western Blot Analysis
Lysate preparation and western blotting analysis were performed as described in Supplemental Data.

Isolation of mRNA, RT-PCR, and qRT-PCR
RNA was analyzed by RT-PCR or quantitative RT-PCR (qRT-PCR). DNA primers and details of the procedure are listed in Supplemental Data.

Retroviral Plasmids, Production, and Infection
MSCV, MSCV-STAT3C, and MSCV-STAT3D (McLemore et al., 2001) were generously provided by D.C. Link (Washington University School of Medicine). Retroviral infection was performed as described previously (Perdiguero et al., 2007). Subconfluent cultures of primary myoblasts were infected by adding medium containing the viral particles, 10 mM HEPES (pH 7.3), and 4 μg/ml of polybrene to each plate. The medium was removed 24 hr later, and the cells were then cultured as indicated.

Histology and Immunohistochemistry
Cryostat sections (10 μm thickness) from plantaris muscles of WT and IL-$6^{-/-}$ mice were obtained before and after overloading at the indicated times. Sections were air dried and stored at −80°C before processing for routine hematoxylin and eosin staining and immunohistochemical analyses. Immunodetection of IL-6, Pax7, MyoD, p-STAT3, myogenin, and eMHC was performed with specific antibodies against IL-6 (AF-406-NA; R&D Systems), Pax7 (PAX7-c; Developmental Studies Hybridoma Bank), MyoD (5.8A; DAKO), p-STAT3 Tyr705 (#9131; Cell Signaling Technology), myogenin (F5D, neat hybridoma supernatant; Developmental Studies Hybridoma Bank), and eMHC (F1652, neat hybridoma supernatant; Developmental Studies Hybridoma Bank). Quantification of the number of myonuclei per myofiber was performed on sections stained with primary specific antibody against dystrophin (MANDYS8; Sigma) and DAPI. Labeling of cryosections with mouse monoclonal primary antibodies was performed using the peroxidase or fluorescein M.O.M. Kit (Vector Laboratories) according to the manufacturer's instructions. Double immunostainings were performed with sequential addition of each primary and secondary antibody, employing appropriate positive and negative controls. Detection of proliferating cells was performed with specific antibodies against BrdU (Oxford Biotech) and p-H3 Ser10 (MC463; Upstate) using intestinal tissue as a positive control. Sections were air dried, kept unfixed (Pax7 and eMHC) or fixed in paraformaldehyde 2%–4%, washed in PBS, and incubated with primary antibodies according to manufacturer's instructions after blocking for 1 hr at room temperature with a high-protein solution in PBS (Vector Laboratories). Subsequently, the slides were washed in PBS and incubated with appropriate secondary antibodies and labeling dyes. After washing, tissue sections were mounted with Vectashield containing DAPI (Vector Laboratories).

Data Collection and Analysis
To measure myofiber cross-sectional area (CSA), plantaris muscles were cut crosswise through the thickest part, and cryostat sections were stained with hematoxylin and eosin. Muscle fiber size analyses; nuclei counts; and quantification of the numbers of Pax7-, BrdU-, MyoD-, p-STAT3-, myogenin-, eMHC-, and p-H3-positive cells were performed on images from muscle cross-sections. Micrographs were obtained using a Leica DMR microscope equipped with a camera, and digitized images taken from different areas of cryosections were analyzed. Individual muscle fibers were outlined and CSA was determined using the image analysis software ImageJ 1.36b (http://rsb.info.nih.gov/ij/). CSA analysis was performed on a total of 6586 myofibers. Myonuclei counts were performed by counting the number of nuclei within the dystrophin-positive sarcolemma outline on pictures taken from control and overloaded plantaris muscles. A total of 2326 fibers from both genotypes were analyzed. The total number of BrdU-positive cells counted outside the dystrophin outline was 6649 and 2649 for overloaded muscles obtained 3 days after surgery from WT and IL-$6^{-/-}$ mice, respectively. No BrdU-positive cells were detected in control muscles. Satellite cell detection was performed by determining the number of Pax7-positive cells on at least four transversal sections obtained at two different locations for each muscle. A total of 369 Pax7-positive cells were analyzed. Data corresponding to the number of MyoD-positive cells in WT and IL-$6^{-/-}$ muscles at 3 days post-CH were obtained after counting 353 and 308 cells, respectively. At this time point, a total of 488 and 210 myogenin-positive cells from WT and IL-$6^{-/-}$ muscles were counted, respectively, whereas the total number of eMHC-positive cells counted was 796 and 306 for WT and IL-$6^{-/-}$ overloaded muscles, respectively.

Differences in fiber CSA were analyzed by nonparametric Wilcoxon signed-ranks test using SPSS software. Statistical differences between pairs of samples were assessed by unpaired two-tailed Student's t test. For all statistical tests, the 0.05 level of confidence was accepted as statistically significant.

Supplemental Data
Supplemental Data include Supplemental Experimental Procedures, Supplemental References, two tables, and seven figures and can be found with this article online at http://www.cellmetabolism.org/cgi/content/full/7/1/33/DC1/.

REFERENCES

Adams, G.R. (2006). Satellite cell proliferation and skeletal muscle hypertrophy. Appl. Physiol. Nutr. Metab. 31, 782–790.

Adams, G.R., Caiozzo, V.J., Haddad, F., and Baldwin, K.M. (2002). Cellular and molecular responses to increased skeletal muscle loading after irradiation. Am. J. Physiol. Cell Physiol. 283, C1182–C1195.

Baeza-Raja, B., and Munoz-Canoves, P. (2004). p38 MAPK-induced nuclear factor-kappaB activity is required for skeletal muscle differentiation: role of interleukin-6. Mol. Biol. Cell 15, 2013–2026.

Banzet, S., Koulmann, N., Sanchez, H., Serrurier, B., Peinnequin, A., Alonso, A., and Bigard, X. (2007). Contraction-induced interleukin-6 transcription in rat slow-type muscle is partly dependent on calcineurin activation. J. Cell. Physiol. 210, 596–601.

Bartoccioni, E., Michaelis, D., and Hohlfeld, R. (1994). Constitutive and cytokine-induced production of interleukin-6 by human myoblasts. Immunol. Lett. 42, 135–138.

Birchmeier, C., and Brohmann, H. (2000). Genes that control the development of migrating muscle precursor cells. Curr. Opin. Cell Biol. 12, 725–730.

Bodine, S.C., Stitt, T.N., Gonzalez, M., Kline, W.O., Stover, G.L., Bauerlein, R., Zlotchenko, E., Scrimgeour, A., Lawrence, J.C., Glass, D.J., and Yancopoulos, G.D. (2001). Akt/mTOR pathway is a crucial regulator of skeletal muscle hypertrophy and can prevent muscle atrophy in vivo. Nat. Cell Biol. 3, 1014–1019.

Bonavaud, S., Charrierre-Bertrand, C., Rey, C., Leibovitch, M., Pedersen, N., Frisdal, E., Planus, E., Blasi, F., Gherardi, R., and Barlovatz-Meimon, G. (1997). Evidence of a non-conventional role for the urokinase tripartite complex (uPAR/uPA/PAI-1) in myogenic cell fusion. J. Cell Sci. 110, 1083–1089.

Carson, J.A., Nettleton, D., and Reecy, J.M. (2002). Differential gene expression in the rat soleus muscle during early work overload-induced hypertrophy. FASEB J. 16, 207–209.

Crescenzi, M., Fleming, T.P., Lassar, A.B., Weintraub, H., and Aaronson, S.A. (1990). MyoD induces growth arrest independent of differentiation in normal and transformed cells. Proc. Natl. Acad. Sci. USA 87, 8442–8446.

Dani, C., Chambers, I., Johnstone, S., Robertson, M., Ebrahimi, B., Saito, M., Taga, T., Li, M., Burdon, T., Nichols, J., and Smith, A. (1998). Paracrine induction of stem cell renewal by LIF-deficient cells: a new ES cell regulatory pathway. Dev. Biol. 203, 149–162.

Darr, K.C., and Schultz, E. (1989). Hindlimb suspension suppresses muscle growth and satellite cell proliferation. J. Appl. Physiol. 67, 1827–1834.

De Rossi, M., Bernasconi, P., Baggi, F., de Waal Malefyt, R., and Mantegazza, R. (2000). Cytokines and chemokines are both expressed by human myoblasts: possible relevance for the immune pathogenesis of muscle inflammation. Int. Immunol. 12, 1329–1335.

Dhawan, J., and Rando, T.A. (2005). Stem cells in postnatal myogenesis: molecular mechanisms of satellite cell quiescence, activation and replenishment. Trends Cell Biol. 15, 666–673.

Endo, T., and Nadal-Ginard, B. (1986). Transcriptional and posttranscriptional control of c-myc during myogenesis: its mRNA remains inducible in differentiated cells and does not suppress the differentiated phenotype. Mol. Cell. Biol. 6, 1412–1421.

Ernst, M., and Jenkins, B.J. (2004). Acquiring signalling specificity from the cytokine receptor gp130. Trends Genet. 20, 23–32.

Forcales, S.V., and Puri, P.L. (2005). Signaling to the chromatin during skeletal myogenesis: novel targets for pharmacological modulation of gene expression. Semin. Cell Dev. Biol. 16, 596–611.

Glass, D.J. (2003). Signalling pathways that mediate skeletal muscle hypertrophy and atrophy. Nat. Cell Biol. 5, 87–90.

Glass, D.J. (2005). Skeletal muscle hypertrophy and atrophy signaling pathways. Int. J. Biochem. Cell Biol. 37, 1974–1984.

Guttridge, D.C., Albanese, C., Reuther, J.Y., Pestell, R.G., and Baldwin, A.S., Jr. (1999). NF-kappaB controls cell growth and differentiation through transcriptional regulation of cyclin D1. Mol. Cell. Biol. 19, 5785–5799.

Haddad, F., Zaldivar, F., Cooper, D.M., and Adams, G.R. (2005). IL-6-induced skeletal muscle atrophy. J. Appl. Physiol. 98, 911–917.

Halevy, O., Novitch, B.G., Spicer, D.B., Skapek, S.X., Rhee, J., Hannon, G.J., Beach, D., and Lassar, A.B. (1995). Correlation of terminal cell cycle arrest of skeletal muscle with induction of p21 by MyoD. Science 267, 1018–1021.

Hiscock, N., Chan, M.H., Bisucci, T., Darby, I.A., and Febbraio, M.A. (2004). Skeletal myocytes are a source of interleukin-6 mRNA expression and protein release during contraction: evidence of fiber type specificity. FASEB J. 18, 992–994.

Horsley, V., Jansen, K.M., Mills, S.T., and Pavlath, G.K. (2003). IL-4 acts as a myoblast recruitment factor during mammalian muscle growth. Cell 113, 483–494.

Jonsdottir, I.H., Schjerling, P., Ostrowski, K., Asp, S., Richter, E.A., and Pedersen, B.K. (2000). Muscle contractions induce interleukin-6 mRNA production in rat skeletal muscles. J. Physiol. 528, 157–163.

Kami, K., and Senba, E. (2002). In vivo activation of STAT3 signaling in satellite cells and myofibers in regenerating rat skeletal muscles. J. Histochem. Cytochem. 50, 1579–1589.

Kamimura, D., Ishihara, K., and Hirano, T. (2003). IL-6 signal transduction and its physiological roles: the signal orchestration model. Rev. Physiol. Biochem. Pharmacol. 149, 1–38.

Kataoka, Y., Matsumura, I., Ezoe, S., Nakata, S., Takigawa, E., Sato, Y., Kawasaki, A., Yokota, T., Nakajima, K., Felsani, A., and Kanakura, Y. (2003). Reciprocal inhibition between MyoD and STAT3 in the regulation of growth and differentiation of myoblasts. J. Biol. Chem. 278, 44178–44187.

Keller, C., Steensberg, A., Pilegaard, H., Osada, T., Saltin, B., Pedersen, B.K., and Neufer, P.D. (2001). Transcriptional activation of the IL-6 gene in human contracting skeletal muscle: influence of muscle glycogen content. FASEB J. 15, 2748–2750.

Kishimoto, T. (2005). Interleukin-6: from basic science to medicine–40 years in immunology. Annu. Rev. Immunol. 23, 1–21.

Kitzmann, M., and Fernandez, A. (2001). Crosstalk between cell cycle regulators and the myogenic factor MyoD in skeletal myoblasts. Cell. Mol. Life Sci. 58, 571–579.

Kiuchi, N., Nakajima, K., Ichiba, M., Fukada, T., Narimatsu, M., Mizuno, K., Hibi, M., and Hirano, T. (1999). STAT3 is required for the gp130-mediated full activation of the c-myc gene. J. Exp. Med. 189, 63–73.

Kopf, M., Baumann, H., Freer, G., Freudenberg, M., Lamers, M., Kishimoto, T., Zinkernagel, R., Bluethmann, H., and Kohler, G. (1994). Impaired immune and acute-phase responses in interleukin-6-deficient mice. Nature 368, 339–342.

Li, Z., Wang, C., Prendergast, G., and Pestell, R.G. (2006). Cyclin D1 functions in cell migration. Cell Cycle 5, 2440–2442.

Masuda, M., Suzui, M., Yasumatu, R., Nakashima, T., Kuratomi, Y., Azuma, K., Tomita, K., Komiyama, S., and Weinstein, I.B. (2002). Constitutive activation of signal transducers and activators of transcription 3 correlates with cyclin D1 overexpression and may provide a novel prognostic marker in head and neck squamous cell carcinoma. Cancer Res. 62, 3351–3355.

McLemore, M.L., Grewal, S., Liu, F., Archambault, A., Poursine-Laurent, J., Haug, J., and Link, D.C. (2001). STAT-3 activation is required for normal G-CSF-dependent proliferation and granulocytic differentiation. Immunity 14, 193–204.

Mourkioti, F., and Rosenthal, N. (2005). IGF-1, inflammation and stem cells: interactions during muscle regeneration. Trends Immunol. 26, 535–542.

O'Connor, R.S., Pavlath, G.K., McCarthy, J.J., and Esser, K.A. (2007). Last Word on Point:Counterpoint: Satellite cell addition is/is not obligatory for skeletal muscle hypertrophy. J. Appl. Physiol. 103, 1107.

Pedersen, B.K., and Fischer, C.P. (2007). Beneficial health effects of exercise–the role of IL-6 as a myokine. Trends Pharmacol. Sci. 28, 152–156.

Penkowa, M., Keller, C., Keller, P., Jauffred, S., and Pedersen, B.K. (2003). Immunohistochemical detection of interleukin-6 in human skeletal muscle fibers following exercise. FASEB J. 17, 2166–2168.

Perdiguero, E., Ruiz-Bonilla, V., Gresh, L., Hui, L., Ballestar, E., Sousa-Victor, P., Baeza-Raja, B., Jardi, M., Bosch-Comas, A., Esteller, M., et al. (2007). Genetic analysis of p38 MAP kinases in myogenesis: fundamental role of p38alpha in abrogating myoblast proliferation. EMBO J. 26, 1245–1256.

Rao, S.S., Chu, C., and Kohtz, D.S. (1994). Ectopic expression of cyclin D1 prevents activation of gene transcription by myogenic basic helix-loop-helix regulators. Mol. Cell. Biol. *14*, 5259–5267.

Rose-John, S. (2003). Interleukin-6 biology is coordinated by membrane bound and soluble receptors. Acta Biochim. Pol. *50*, 603–611.

Rosenblatt, J.D., and Parry, D.J. (1992). Gamma irradiation prevents compensatory hypertrophy of overloaded mouse extensor digitorum longus muscle. J. Appl. Physiol. *73*, 2538–2543.

Rosenblatt, J.D., and Parry, D.J. (1993). Adaptation of rat extensor digitorum longus muscle to gamma irradiation and overload. Pflugers Arch. *423*, 255–264.

Rosenblatt, J.D., Yong, D., and Parry, D.J. (1994). Satellite cell activity is required for hypertrophy of overloaded adult rat muscle. Muscle Nerve *17*, 608–613.

Schiaffino, S., and Serrano, A. (2002). Calcineurin signaling and neural control of skeletal muscle fiber type and size. Trends Pharmacol. Sci. *23*, 569–575.

Sorrentino, V., Pepperkok, R., Davis, R.L., Ansorge, W., and Philipson, L. (1990). Cell proliferation inhibited by MyoD1 independently of myogenic differentiation. Nature *345*, 813–815.

Tisdale, M.J. (2005). The ubiquitin-proteasome pathway as a therapeutic target for muscle wasting. J. Support. Oncol. *3*, 209–217.

Turkson, J., Ryan, D., Kim, J.S., Zhang, Y., Chen, Z., Haura, E., Laudano, A., Sebti, S., Hamilton, A.D., and Jove, R. (2001). Phosphotyrosyl peptides block Stat3-mediated DNA binding activity, gene regulation, and cell transformation. J. Biol. Chem. *276*, 45443–45455.

Turner, D.C., Lawton, J., Dollenmeier, P., Ehrismann, R., and Chiquet, M. (1983). Guidance of myogenic cell migration by oriented deposits of fibronectin. Dev. Biol. *95*, 497–504.

Viswanathan, S., Benatar, T., Rose-John, S., Lauffenburger, D.A., and Zandstra, P.W. (2002). Ligand/receptor signaling threshold (LIST) model accounts for gp130-mediated embryonic stem cell self-renewal responses to LIF and HIL-6. Stem Cells *20*, 119–138.

Wei, Q., and Paterson, B.M. (2001). Regulation of MyoD function in the dividing myoblast. FEBS Lett. *490*, 171–178.

Wells, J.M., and Strickland, S. (1997). Regulated localization confers multiple functions on the protease urokinase plasminogen activator. J. Cell. Physiol. *171*, 217–225.